



OPEN Choroidal thickness as predictor of subclinical carotid atherosclerosis in adults with type 1 diabetes

Esmeralda Castelblanco¹, Ignacio Salvador-Miras², Marc Carbonell³, Mònica Gratacòs⁴, Alicia Traveset⁵, Eudald Correig⁶, Marta Hernández⁷, Núria Alonso^{8,9,10}, Josep Franch-Nadal^{4,10} & Dídac Mauricio^{2,10,11,12}✉

Patients with Type 1 Diabetes (T1DM) have a higher risk of cardiovascular disease. This study used carotid ultrasound to identify subclinical carotid plaques and Optical Coherence Tomography (OCT) to evaluate ophthalmological markers as predictors of carotid plaque presence in 242 adults with T1DM, employing machine learning models for early risk assessment. Individuals with carotid plaques ($N=67$) did not show significant differences in retinal nerve fiber layer (RNFL) and ganglion cell layer (GCL) and inner plexiform layer (IPL) complex compared to those without ($N=175$). However, subfoveal and temporal choroidal area thickness significantly decreased in individuals with plaques ($P \leq 0.01$). Machine learning identified age, hypertension, dyslipidemia, smoking, and diabetic retinopathy as key predictors for plaque presence, while ophthalmological measures made a modest contribution. Choroidal thickness exhibited an inverse relationship with plaque risk. Despite robust accuracy and high specificity (82–85% and 92–98%, respectively), the models were overly conservative in predicting positive instances (balanced accuracy of 0.60 for the left eye and 0.71 for the right eye). If further validated, choroidal thickness could complement traditional risk factors as an early marker of CV risk in T1DM patients. Integrating this measure in specialized clinical settings could help identify individuals who may need additional cardiovascular assessments.

Keywords Type 1 diabetes mellitus, Carotid artery plaque, Subclinical atherosclerosis, Cardiovascular risk, Optical coherence tomography, Choroid thickness, Machine learning

Diabetes mellitus (DM) stands as a prominent risk factor for cardiovascular disease (CVD), implicated in accelerating the progression of the atherosclerotic process¹. The risk of CVD in T1DM patients is approximately 10 times higher than in the general population, accounting for 44% of disease-related deaths². Moreover, premature atherosclerosis is a leading cause of death in T1DM adults, particularly those with microvascular complications³.

Atherosclerosis progresses from an early, unnoticed phase, known as subclinical or asymptomatic atherosclerosis (SCA), to overt clinical CVD⁴. Early detection of SCA is crucial as it helps predict future CV events and offers opportunities for intervention to prevent disease progression^{5,6}.

Screening methods to assess SCA manifestations include imaging surrogate markers, notably carotid ultrasound (US). This non-invasive method can detect increased arterial wall thickness (carotid intima-media thickness, cIMT) or the presence of carotid plaques^{7,8}. There is strong evidence that patients with DM

¹Department of Medicine, Division of Endocrinology, Metabolism and Lipid Research, Washington University School of Medicine, St Louis, MO 63110, USA. ²Department of Endocrinology & Nutrition, Hospital de la Santa Creu i Sant Pau, Sant Quintí, 89, 08041 Barcelona, Spain. ³Department of Ophthalmology, Germans Trias i Pujol University Hospital, 08916 Badalona, Spain. ⁴DAP-Cat group, Unitat de Suport a la Recerca Barcelona, Fundació Institut Universitari per a la recerca a l'Atenció Primària de Salut Jordi Gol i Gurina (IDIAPJGol), 08007 Barcelona, Spain. ⁵Department of Ophthalmology, Arnau de Vilanova University Hospital and Lleida Biomedical Research Institute (IRBLleida), 25198 Lleida, Spain. ⁶Department of Biostatistics, Universitat Rovira i Virgili, 43201 Reus, Spain. ⁷Department of Endocrinology & Nutrition, Hospital Universitari Arnau de Vilanova & Institut d'Investigació Biomèdica de Lleida (IRB Lleida), 25198 Lleida, Spain. ⁸Department of Endocrinology & Nutrition, Germans Trias i Pujol University Hospital, 08916 Badalona, Spain. ⁹Department of Medicine, Autonomous University of Barcelona, 08193 Barcelona, Spain. ¹⁰CIBER de Diabetes y Enfermedades Metabólicas Asociadas, Instituto de Salud Carlos III, 28029 Madrid, Spain. ¹¹Institut d'Investigació Biomèdica Sant Pau (IIB Sant Pau), 08041 Barcelona, Spain. ¹²Faculty of Medicine, University of Vic (UVIC/UCC), 08500 Vic, Spain. ✉email: didacmauricio@gmail.com

have an increased cIMT and a greater burden of plaques^{9,10}. Arterial wall thickening is not only observed in T1DM patients with microvascular complications such as retinopathy and nephropathy but also in those with uncomplicated disease, individuals with a short disease duration, and adults recently diagnosed with T1DM¹¹.

Underlying carotid artery disease (CAD) often impacts retinal health, a connection underscored by the retina's extensive vascularity, which is essential as it is the tissue with the highest metabolic demands in the body^{12,13}. The eye's blood supply relies on a complex network of arteries originating from the retinal and choroidal vasculature, both derived from the ophthalmic artery, the primary branch of the ipsilateral internal carotid artery (ICA)¹⁴. Consequently, changes in blood flow parameters within the ICA can lead to retinal emboli stemming from atherosclerotic plaques or retinal and choroidal hypoperfusion due to ICA stenosis¹². At the clinical level, this may translate into severe ophthalmological complications that range from transient monocular visual loss (amaurosis fugax) to complete blindness due to central retinal artery occlusion or anterior ischemic optic neuropathy caused by hypoperfusion of the optic nerve head¹².

Optical coherence tomography (OCT) is a valuable non-invasive imaging technique that provides detailed, cross-sectional morphological imaging of the retina, vitreous, choroid, and optic nerve alternative or complement to traditional fluorescein angiography¹⁵. Studies based on OCT scans have shown that the presence of CAD and ICA stenosis decreases choroid thickness, suggesting that individuals with abnormally thin subfoveal choroidal thickness, even in the absence of ocular disease, may benefit from carotid artery screening for asymptomatic carotid artery stenosis¹⁶. Similarly, OCT studies in T1DM patients indicate that thinning of the RNFL may occur even in the absence of overt microvascular vascular changes such as diabetic retinopathy (DR)^{17–27}, though findings on choroidal thickness remain inconclusive^{25–32}. Interestingly, retinal microvascular changes may also reflect early macrovascular damage, as evidenced by a study linking increased cIMT with wider retinal arteriolar and venular calibers in T1DM patients without DR³³. This connection between subclinical atherosclerosis and retinal changes highlights the potential of OCT in early cardiovascular risk detection. However, to the best of our knowledge, there has been a lack of subsequent research or independent verification to validate these results.

In this scenario, we hypothesized that OCT-derived parameters differ in relation to the presence of subclinical atherosclerosis in patients with T1DM, reflecting both macrovascular changes, such as carotid plaque burden, and microvascular changes, such as those associated with DR. Moreover, we anticipated that these parameters could improve the predictive potential for detecting the presence of carotid plaque in these patients. To address this hypothesis, we compared retinal and choroid thickness obtained from OCT scans in adult subjects with T1DM with and without subclinical atherosclerosis, determined by the presence of carotid plaque through US examination. Moreover, we used machine learning models to identify hidden patterns and complex non-linear interactions between ophthalmological metrics and established demographic and blood markers that could enhance the predictive capability for detecting the presence of carotid plaque.

Methods

Study design and participants

This was a post-hoc analysis of a previous study designed to assess the association of subclinical carotid atherosclerosis and diabetic retinopathy in subjects with T1DM^{25,34}. In the original study, 340 adults diagnosed with T1DM were recruited from two university hospitals within the same public health organization in the Catalonia region of Spain. Inclusion criteria comprised a diabetes duration exceeding one year, normal renal function (defined as estimated glomerular filtration rate [eGFR] > 60 mL/min/1.73 m²), urine albumin excretion rate < 300 mg/g, and an absence of established CVD (including ischemic heart disease, cerebrovascular disease, peripheral arterial disease, and heart failure) or diabetic foot disease. Exclusion criteria included specific ophthalmological conditions: media opacities that hindered a complete eye examination (cataract, corneal opacity, or hemovitreal); refractive error ≥ 5 diopters; concomitant retinal diseases such as choroidal neovascularization, macular geographic atrophy, and retinal vein obstruction; eye inflammation; glaucoma; eye surgery within the year preceding the exam; and laser photocoagulation in the six months before the examination or panphotocoagulation-treated proliferative diabetic retinopathy. Additionally, no patient included in the study had diabetic macular oedema (DME), a condition common in diabetic retinopathy that could affect retinal thickness measurements.

The Local Ethics Committee of both (EC) participating centers approved the original study protocol, and all the participants signed informed consent forms. As the proposed subanalysis did not deviate from the study's objectives, there was no need to resubmit the project as an amendment to the EC. All methods were carried out in accordance with relevant guidelines and regulations, and the study was conducted in accordance with the Declaration of Helsinki.

Clinical and demographic variables

Demographic and clinical information for each participant included age, sex, weight, smoking habits, height, body mass index (BMI), and waist circumference. Hypertension and dyslipidemia were defined as a recorded clinical diagnosis, corroborated by documentation of current antihypertensive and lipid-lowering medication use in the patient's clinical records. The subjects' blood pressure (mean of 2 measurements, 5 min apart) was measured after 10 min in the seated position using a blood pressure monitor (HEM-7001E, Omron, Barcelona, Spain). Biochemical variables derived from fasting serum samples consisted of the lipid profile, including total cholesterol, low-density lipoprotein cholesterol (LDL-c) estimated using the Friedewald formula, high-density lipoprotein cholesterol (HDL-c), and triglycerides, serum creatinine, and eGFR calculated according to Chronic Kidney Disease Epidemiology Collaboration equation³⁵. Additionally, the hemoglobin A1c (HbA1c) levels were determined by high-performance liquid chromatography (HPLC). The urine albumin-to-creatinine ratio (UACR) was determined by analyzing urine samples to quantify creatinine and urine albumin, measured using an immunoturbidimetric method.

Ophthalmological examination

All participants underwent a complete eye examination conducted by an experienced ophthalmologist (M.C). According to the Early Treatment Diabetic Retinopathy Study (ETDRS)³⁶, diabetic retinopathy (DR) was reclassified into five stages: (1) no apparent retinopathy, (2) mild non-proliferative retinopathy (NPDR), (3) moderate NPDR, (4) severe NPDR, and (5) proliferative RD.

The methodology for OCT has been previously detailed in a publication²⁵. Briefly, spectral-domain OCT (SD-OCT) was used to visualize and quantify the thickness of different layers of the retina, namely the RNFL and the ganglion cell layer/ inner plexiform layer (GCL/IPL) complex. RNFL thickness was assessed following the Optic Disc Cube 200 × 200 protocol, with automatic quadrant-wise data calculation (temporal, superior, nasal, and inferior sectors). The GCL and minimum GCL thickness were measured using the Macula Cube 512 × 128 protocol centered around the fovea. Enhanced-depth imaging OCT (EDI-OCT) was used to precisely measure choroidal thickness employing a high-definition 5-line Raster scan pattern. Manual measurements were performed with a caliper in three positions (subfoveal, nasal, and temporal to the fovea) at a distance of 2000 µm. Choroidal thickness was computed as the vertical distance between the first hyperreflective line (Bruch's membrane) and the second hyperreflective line (the internal surface of the sclera)³⁷.

Carotid vascular ultrasound scanning

A dedicated researcher conducted the carotid US examination at each participating centre. The comprehensive methodology for the US imaging technique has been previously documented^{34,38}. In brief, the intima-media-adventitial thickness (IMT) was evaluated according to a standardized protocol, defined as the distance between the lumen-intima and media-adventitial ultrasound interfaces (intima-media complex). The measurements were performed using semi-automated software to ensure consistency and accuracy. The mean IMT and mean-maximum IMT were computed for both the right and left-side carotid artery across three segments: common carotid, carotid bulb, and internal carotid. Atherosclerotic plaques within the same regions were identified through B-mode and color Doppler examinations in both longitudinal and transverse views. Plaques were defined as a "focal structure invading the arterial lumen, encompassing at least 0.5 mm or 50% of the surrounding cIMT value, or demonstrating a thickness of 1.5 mm, measured from the interference of the media-adventitia to the leading edge of the intima-lumen." This definition aligns with the criteria outlined in the Mannheim consensus³⁹.

Statistical analysis

Descriptive statistics were computed for quantitative variables with normal or non-normal distributions, expressed as mean (standard deviation) or median (interquartile range). Qualitative variables were presented in terms of absolute and relative frequencies. The normal distribution was assessed using the Shapiro-Wilk's test. Group differences were examined using Student's t-test, analysis of variance (ANOVA), Mann-Whitney's, and Kruskal-Wallis' tests for quantitative variables based on their distribution. For qualitative variables, differences were assessed using the appropriate Chi-square test or Fisher's exact test.

Machine learning

Given the dependence of retinal and choroidal irrigation on the ipsilateral carotid, we conducted separate machine learning models for each carotid with its ipsilateral eye. The outcome variable was the presence of carotid plaque in any of the carotid artery segments, and the predicting variables included all features encompassing demographic and clinical data and OCT-derived retinal and choroidal measures. All missing values in each of the two datasets (left and right side) were imputed using the Multiple Imputation by Chained Equations (MICE) missing data imputation method⁴⁰.

We employed three distinct classifiers: Random Forest, Gradient Boosting, and a logistic model regularized via elastic net to prevent overfitting. Model parameters were fine-tuned using 5-fold cross-validation over 100 combinations of hyperparameters. For model development, our dataset was randomly divided into a training set (80% of patients) for constructing models and a test set (20%) for evaluating model performance. To assess the impact of predictive variables, we determined their relative importance through out-of-bag accuracy before and after variable permutation for the best model between Random Forests and boosted models. These two models were chosen for their accuracy in handling complex scenarios⁴¹. Additionally, we performed regularized logistic regressions to ascertain whether each variable exerted a protective or harmful effect on the presence of carotid plaque. The direction of the effect was evaluated based on the sign of the coefficient.

To assess the predictive capabilities of the models, we constructed confusion matrices to derive basic metrics, including sensitivity, specificity (or recall), positive predictive value (PPV or precision), and negative predictive value (NPV). As summary metrics, we computed the accuracy, the area under the receiver-operating characteristic curve (AUROC), and the area under the precision-recall curve (AUPR or average precision). Note that ROC curves might not be optimal for assessing performance in datasets with significant class imbalance and AUPR is a preferred metric for unbalanced data. This preference arises because AUPR focuses specifically on the positive class, a critical consideration when this class constitutes a relatively small fraction of the population^{42,43}. To address this limitation, we also computed the balanced accuracy (calculated as the average of sensitivity and specificity), which is a performance metric that accounts for uneven class distributions^{42,43}.

All data processing and statistical analyses were performed with the R statistical computing software (version 4.1.0). A two-sided p-value < 0.05 was considered statistically significant in all analyses.

Results

Baseline characteristics

Out of the initial sample of 340 subjects with T1DM, 98 individuals were excluded from the study due to the unavailability of OCT image data or ophthalmologic exclusion criteria (Supplementary Fig. S1 online). Of the resulting cohort of 242 patients, 92 (38%) presented with subclinical atherosclerotic plaques. Specifically, 67 (72.8%) of subjects presented with carotid plaques, located in either the common, bulb, or internal segments of the carotid artery, whereas 72 subjects (79.1%) showed femoral plaques (Supplementary Fig. S1 online). Additionally, half of the patients had both femoral and carotid plaques concurrently.

Half of the patients with carotid plaques exhibited multiple plaques, with a median count of 2 (interquartile range, 1.0–2.0) (Table 1). Patients showing carotid plaques were older than those without plaques (mean age 51 vs. 41 years; $P < 0.001$), had a longer T1DM duration (21 vs. 18 years; $P = 0.011$), and slightly higher BMI (median 25.9 vs. 24.7 kg/m²; $P = 0.021$) (Table 1). However, no significant differences were observed between the groups regarding sex or glycemic control. In terms of comorbidities, individuals with plaques had a higher prevalence of hypertension (55.2% vs. 12.0%; $P < 0.001$), current or former smoking habits ($P = 0.009$), dyslipidemia (71.6 vs. 26.9%; $P < 0.001$), worse renal function (eGFR and UACR, $P < 0.001$ and $P = 0.018$, respectively), and a higher frequency of DR (59.7% vs. 36%; $p < 0.001$), with most patients in both groups classified as having mild NPDR.

Association between OCT ophthalmological measures and carotid plaque

In the comparative analysis of ophthalmological variables derived from SD-OCT scans (Supplementary Table S1 and Fig. 1), no notable differences emerged in the median thickness of peripapillary RNFL and macular GCL-IPL areas between individuals with and without carotid plaques, considering the laterality of eyes. In contrast, EDI-OCT scans showed a significant decrease in the median subfoveal and temporal choroidal area thickness among individuals with carotid plaques for both eyes (all $P \leq 0.01$) (Supplementary Table S1 and Fig. 2). Furthermore, while a significant reduction in nasal choroidal thickness was observed exclusively in the left eye ($P < 0.01$), there was also a notable trend toward lower nasal choroidal thickness in patients with carotid plaques, although this difference did not reach statistical significance (Fig. 2).

Contribution of OCT ophthalmological measures to carotid plaque prediction using machine learning-based models

In our machine learning models, including both the demographic, clinical, and ophthalmological features, age, hypertension, and dyslipidemia were the variables with the most significant weight for making accurate predictions (highest variable importance scores) for the presence of carotid plaque for both eyes (Fig. 3a and b). Ophthalmological measures made a relatively modest contribution to the model; however, all choroidal thickness parameters were consistently ranked among the top 11 variables for both eyes, accounting for 8–10% of the variable importance for the left eye and up to $\geq 25\%$ for the right eye. Furthermore, temporal RFNL emerged prominently among the top 10 variables for the right eye.

The results of the regularized regression analyses showed that age, hypertension, dyslipidemia, smoking habit, and the presence of DR were the most important predictors, collectively pointing to an increased risk of developing carotid plaque, whether on the right or left side (Fig. 3c and d). In contrast, most of the coefficients associated with OCT quantitative measures tended to converge near zero, indicating a marginal impact on the overall risk of carotid plaque. However, a distinctive pattern emerged for all choroidal thickness measures: nasal, temporal, and subfoveal. After accounting for other variables, their effect sizes ranged from small to moderate, showing an inverse relationship with the risk of carotid plaque, with reduced thickness in these areas associated with an elevated risk, a trend observed for both the right and left sides.

Models' performance

The confusion matrix of the classifiers and the prediction plots for each side are shown in Fig. 4. The AUROC values for carotid plaque prediction were robust, measuring 0.82 (95% CI = 0.77–0.87) for the left side and 0.85 (95% CI = 0.76–0.94) for the right side, suggesting excellent discriminatory power. However, it's essential to note that our dataset exhibited an imbalance, with a notable overrepresentation of negative cases (no carotid plaque). Balanced accuracy, a metric tailored for such scenarios, indicated reasonable effectiveness, with scores of 0.71 for the left eye and 0.60 for the right eye. However, when using the average precision (AUPR), a key metric for imbalanced datasets, the values were comparatively low (0.51 for the left eye and 0.43 for the right eye). Upon closer inspection of the confusion matrices and prediction plots (Fig. 4), it became evident that the algorithms exhibited limitations in identifying positive samples, marked by low sensitivity. Specifically, the models achieved 63% and 75% accuracy in correctly identifying positive instances (PPV) for the left and right eye, respectively. In contrast, the models' performance in correctly identifying true negatives (NPV) was robust, exceeding 85% on each side.

Discussion

The present study investigated how OCT measures showing predictive potential for subclinical atherosclerosis may extend their applicability to T1DM patients. The results showed that almost all choroidal measures were significantly reduced in patients with carotid plaques in the subclinical stage compared to those without plaques. The machine learning models based on traditional risk factors and OCT-derived ophthalmological measures identified age, hypertension, dyslipidemia, smoking, and DR as the most significant independent predictors of ipsilateral carotid plaque. While ophthalmological measures collectively made a relatively modest contribution to the models, reduced choroidal thickness was identified as a predictor of carotid plaque. The models exhibited robust discriminatory power but faced challenges in accurately identifying positive instances within

	No carotid plaque N = 175	Carotid Plaque N = 67	P-value
Age, years, median [P25-P75]	41.0 [36.0;47.0]	51.0 [47.0;59.5]	< 0.001
Sex, male, n (%)	80 (45.7%)	34 (50.7%)	0.577
HbA1c, %, median [P25-P75]	7.40 [6.95;8.00]	7.60 [7.00;8.20]	0.205
Diabetes duration, years, median [P25-P75]	18.0 [13.0;26.0]	21.0 [15.0;32.0]	0.011
BMI, kg/m ² , median [P25-P75]	24.7 [22.1;27.4]	25.9 [23.5;28.2]	0.021
Waist circumference, cm, median [P25-P75]	87.0 [79.0;96.0]	90.0 [84.0;97.0]	0.098
Comorbidities			
Hypertension, n (%)	21.0 (12.0%)	37.0 (55.2%)	< 0.001
SBP, mmHg, median [P25-P75]	121.0 [112;133]	135.0 [126;144]	< 0.001
DBP, mmHg, median [P25-P75]	74.0 [68–80]	76.0 [69–82]	0.489
Smoking, n (%)			0.009
No	93 (53.1%)	21 (31.3%)	
Yes	40 (22.9%)	24 (35.8%)	
Former	42 (24.0%)	22 (32.8%)	
Dyslipidemia, n (%)	47 (26.9%)	48 (71.6%)	< 0.001
Lipid profile, mg/dL, median [P25-P75]			
Total cholesterol	177.0 [161–200]	178.0 [162–196]	0.764
HDL cholesterol	63.0 [53–74]	61.0 [53–76]	0.995
LDL cholesterol	102.0 [86–119]	97.4 [81.5–110.2]	0.719
Triglycerides	64.0 [51–84]	71.0 [56–89]	0.042
Renal function, median [P25-P75]			
Serum Creatinine, mg/dL	0.75 [0.65–0.86]	0.76 [0.67–0.90]	0.435
eGFR, mL/min/1.73 m ²	106.7 [98.4–115.1]	97.9 [90.0–105–8]	< 0.001
Urine albumin/creatinine ratio, mg/g, median [P25-P75]	3.58 [1.80;5.64]	4.82 [2.85;7.16]	0.018
Ophthalmologic examination			
Diabetic retinopathy (DR), n%			< 0.001
No DR	112 (64.0)	27 (40.3)	
Mild non-proliferative DR	49 (77.8)	25 (62.5)	
Moderate non-proliferative DR	5 (7.9)	10 (25.0)	
Severe non-proliferative DR	9 (14.3)	5 (12.5)	
Proliferative DR	0 (0.0)	0 (0.0)	
Ultrasonographic study*			
cIMT, mm			< 0.001
Median [P25-P75]	0.61 [0.5–0.7]	0.68 [0.6–0.8]	
Mean (SD)	0.61 (0.1)	0.68 (0.1)	
Right cIMT, mm			< 0.001
Median [P25-P75]	0.60 [0.5–0.7]	0.67 [0.6–0.7]	
Mean (SD)	0.61 (0.1)	0.67 (0.1)	
Left cIMT, mm			< 0.001
Median [P25-P75]	0.61 [0.5–0.7]	0.67 [0.6–0.8]	
Mean (SD)	0.62 (0.1)	0.69 (0.1)	
Presence and burden of carotid plaques, n (%)			
Right plaque	–	43 (64.2)	
Left plaque	–	53 (79.1)	
Continued			

	No carotid plaque N = 175	Carotid Plaque N = 67	P-value
Right and left plaque	–	29 (43.3)	
Number of carotid plaques			
Median [P25–P75]	–	2.0 [1.0–2.0]	
One plaque, n (%)	–	33 (49.3)	
Multiple plaques, n (%)	–	34 (50.7)	

Table 1. Comparison of clinical and ultrasonographic characteristics between patients with and without carotid plaque. *Includes plaques in either the common, bulb, or internal segments of the carotid artery. BMI, body mass index; cIMT, carotid intima-media thickness; eGFR, estimated glomerular filtration rate based on the CKD-EPI equation; DBP, diastolic blood pressure; HbA1c, glycated hemoglobin; HDL-c, high-density lipoprotein cholesterol; LDL-c, low-density lipoprotein cholesterol; NPDR, nonproliferative diabetic retinopathy; P25–P75, 25th percentile (P25) and 75th percentile (P75); SBP, systolic blood pressure; US, ultrasound.

an imbalanced dataset. Despite this limitation, the models demonstrated effectiveness in correctly identifying negative instances.

The prevalence of US-evaluated carotid artery plaques in our T1DM population was 27.6%, which is in line with other studies conducted in adult T1DM patients, widely ranging from 11–30%^{44–46}. The profile of patients with plaque comprised older individuals with a longer duration of T1DM, more frequently current or former smokers, with DR, hypertension, dyslipidemia, and normal but comparatively worse renal function. All these factors are well-established traditional risk factors associated with carotid atherosclerosis in the general population⁴⁷, with atherosclerosis in individuals with T1DM³, and align with findings of studies comparing young subjects with T1DM and subclinical arterial damage compared to healthy controls¹¹. However, we did not observe differences regarding HbA1c levels between groups. Data regarding the association between HbA1c and the presence of carotid plaques are limited and inconsistent, with some studies reporting an association with incident carotid plaque or increased cIMT^{48–50} while others do not^{51,52}. These inconsistencies may be attributed to the progressive nature of coronary plaque formation, which involves long-term and progressive narrowing of the carotid artery. Therefore, the timing of the assessment of cIMT or plaque may play a crucial role in determining the association.

In our study, the only OCT-derived measures significantly different between patients with and without carotid plaques in the bivariate analysis were related to the choroid thickness. In contrast, retinal layers, including RFNL and the GCL-IPL complex, demonstrated similar values between the two groups. Thinner RFNL and GCC layers have been inversely correlated with the severity of DR in T1DM^{25,53}, and decreased in patients with minimal or no evidence of DR in many studies^{17–27}, although other studies found no difference^{54,55}. A possible explanation for the discrepancy between these studies and our results regarding GCL and IPL was that we assessed them as one layer due to the technical difficulty of correctly separating them. As such, the slight thickening of the IPL might have been masked by a more pronounced thinning of the GCL⁵⁶. Indeed, a study conducted in adult T1DM patients assessed by OCT found a significant thinning of the RNFL and GCL layers over time, whereas IPL showed a slight but significant thickening, with more pronounced changes associated with the presence or development of DR for all layers⁵⁶. The authors stated that, after eliminating studies looking at the GCL-IPL complex as a whole, the significance of the selective IPL thinning disappeared for most studies⁵⁶.

The observed absence of an association with retinal layers but a reduction in choroidal thickness in the presence of carotid plaques may be attributed to the distinct metabolic needs and vascularity of the inner and outer layers of the retina. The retinal inner layers (RFNL and the GCL-IPL complex) rely on the retinal circulation, characterized by relatively low blood flow and increased hypoxia compared to the outer retina^{13,57}. Indeed, the choroidal circulatory system predominantly supplies the outer retina, contributing to 85% of ocular blood flow^{13,57}. Therefore, changes related to subclinical atherosclerosis might not significantly affect the metabolic demands or structural integrity of the inner retinal layers, although they remain very sensitive to diabetes-induced metabolic stress and result in neuronal cell loss when compromised^{13,57}. Conversely, the observed decrease in choroidal thickness may indicate alterations in the vascular supply to the outer retina, suggesting that changes in blood flow parameters, potentially associated with carotid artery disease, could impact the choroidal vasculature. This would align with the results from OCT studies showing that the reduced ipsilateral choroid thickness present in patients with CAD improves after endarterectomy, which restores choriocapillaris perfusion, correcting this impairment and leading to an increase in thickness^{58,59}.

The integration of machine learning methods is a valuable complement to traditional clinical approaches, such as multiple logistic regression modeling, in identifying biomarkers⁶⁰. This approach offers distinct advantages over conventional methods, including the ability to capture hidden and non-linear interactions, thereby enhancing the accuracy of risk prediction, automatically assessing feature importance, and efficiently handling large datasets⁶⁰. In our study, the models identified age, hypertension, dyslipidemia, smoking, and DR as the top predictors of carotid plaques. These findings align with previous research employing learning-machine models to predict the formation of carotid plaques or identify asymptomatic carotid atherosclerosis^{61–63}. The machine-learning models also indicated that the only ophthalmological parameters contributing to the prediction of plaque were those regarding choroid thickness, particularly in the subfoveal area. These parameters made a

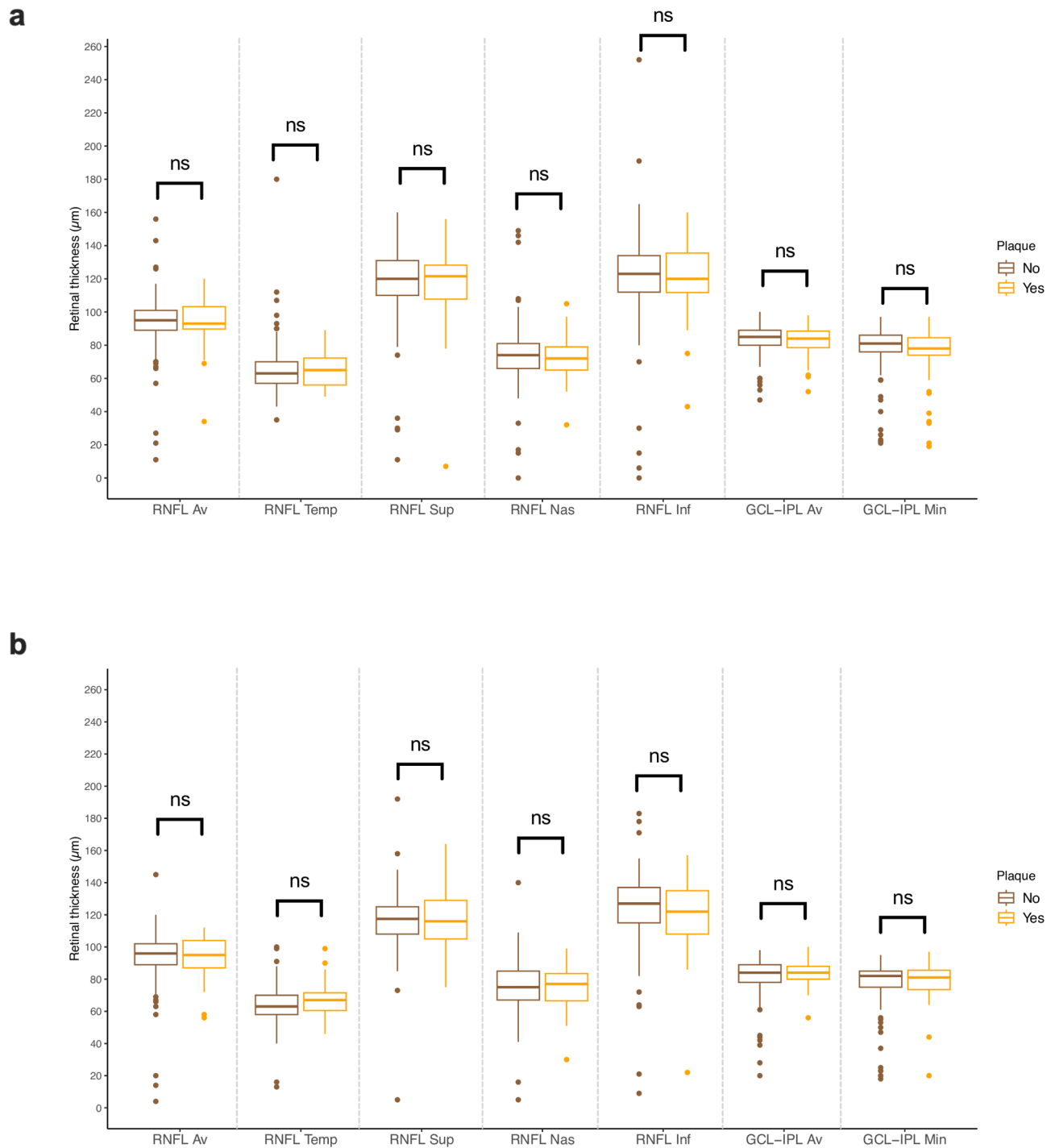


Fig. 1. Comparison of SD-OCT retinal thickness measurement areas between patients with and without plaque for the left eye (a) and the right eye (b). Av, average; GCL-IPL ganglion cell layer-inner plexiform; Inf, inferior; Min, minimum; Nas, nasal; RNFL, retinal nerve fiber layer; Sup, superior; Temp, temporal.

relatively modest to moderate contribution to the overall model predictions, revealing that reduced thickness in these areas was linked to an elevated risk – a consistent trend observed for both the right and left sides. The choroid is thickest subfoveally to meet the high metabolic demands of the avascular fovea, which receives nutrition through the diffusion of the choroid capillaries^{13,57}. Consequently, in scenarios involving compromised blood flow, such as those associated with subclinical carotid plaque, it is unsurprising that choroid thickness is primarily impacted in the subfoveal region^{64–66}.

Subfoveal thickness has been described to be thicker in patients with DM and DR than in those without DR⁶⁷. In a prior study involving the same patient cohort as in the present investigation, our group found that choroid thickness was increased in T1DM subjects with mild or no DR compared to age-matched controls and subjects

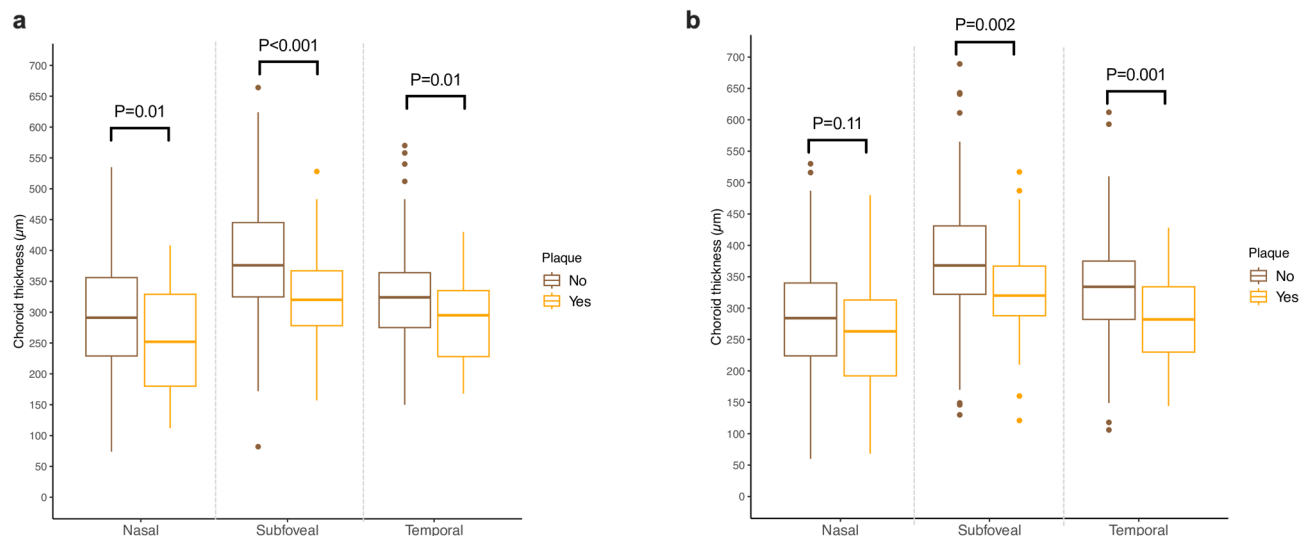


Fig. 2. Comparison of EDI-OCT choroid thickness measurement areas between patients with and without plaque for the left eye (a) and the right eye (b).

with advanced DR²⁵. Within our subsample of T1DM patients with carotid plaque, the models identified DR as one of the most important clinical predictors of carotid plaque, aligning with a systematic review indicating an increased likelihood of DR when there is US evidence of carotid disease, and vice versa⁶⁸. The fact that both DR and reduced choroid thickness independently predicted an elevated risk of carotid plaque reinforces the notion that DR and changes in the choroid structure are tightly coupled phenomena or co-exist in the presence of plaques. These findings suggest that both factors could serve as potential biomarkers for carotid stenosis^{16,68,69}.

The confusion matrix and performance indicators of our models performed well overall with high accuracy (82–85%) and high specificity (92–98%) but a moderate PPV (63–75% precision). This means that the models were overly conservative in predicting positive instances while avoiding making false positive errors. This could be due to the small sample size and unbalanced ratio of patients with and without plaque in the test set⁴². However, additional metrics tailored for imbalanced datasets, such as balanced accuracy (0.60 for the left eye, 0.71 for the right eye), indicated that the models performed above random chance (0.5) and were reasonably effective. The AUPR values (0.43–0.51) also indicated that the models faced difficulties in accurately identifying positive instances despite well-balanced accuracy. Another study evaluated the effectiveness of different machine-learning models to predict asymptomatic carotid atherosclerosis (defined as a cIMT ≥ 1.0 mm or plaque formation) incorporating 19 demographic and blood parameters as inputs from 18,441 subjects⁶². Similar to our findings, the models demonstrated high specificity, ranging between 72% and 88%. However, the sensitivity was lower, ranging between 37% and 53%, and the PPV was between 51.2% and 71%. Although the sample size was much larger than ours, our model, which included both clinical and ophthalmological variables, showed accuracy metrics comparable or even superior to a model relying solely on clinical and demographic variables.

The main strength of our study is that we provide, for the first time, a comprehensive exploration of OCT-derived ophthalmological measures in the context of carotid plaque prediction in patients with T1DM using machine-learning strategies. While coronary angiography remains the gold standard for diagnosing CAD due to its ability to provide direct visualization of coronary anatomy and precise identification of stenotic lesions, it has inherent limitations, particularly in asymptomatic populations⁷⁰. Its invasive nature, higher cost, and procedural risks limit its applicability for widespread screening or the assessment of systemic atherosclerosis. In contrast, carotid US serves as a non-invasive, widely available, and cost-effective tool for evaluating subclinical atherosclerosis and detecting early vascular changes associated with increased cardiovascular risk, making it a valuable surrogate marker for systemic atherosclerotic burden⁷¹.

Notably, our analysis extended beyond the conventional scope by encompassing a diverse array of factors, ranging from traditional risk factors to ophthalmological features to allow for a multifaceted analysis. However, the results of the present study must be interpreted in the context of several limitations. Firstly, the cross-sectional nature of the study limits our ability to establish causal relationships and prevents the assessment of the temporal dynamics of the observed associations. Secondly, the sample size was relatively small, comprising 67 subjects with carotid plaques out of a total of 242 patients. This limited sample size may have increased the risk of both Type I errors and Type II errors in the bivariate analysis. This is evident in the observed asymmetry in the statistical significance regarding nasal choroidal thickness reduction: the left eye showed a significant reduction, whereas the right eye only demonstrated a trend. However, the consistent reduction in both subfoveal and temporal choroidal thicknesses across both eyes in individuals with carotid plaques reinforces the likelihood of a true effect despite the variability in significance levels. Moreover, the small sample size could have adversely impacted the robustness of the machine-learning models. Indeed, a relatively low representation of positive cases can lead to a skewed learning process, where the models may become overly conservative in predicting positive instances⁴². Given the limitations of a small sample size, our findings should be interpreted

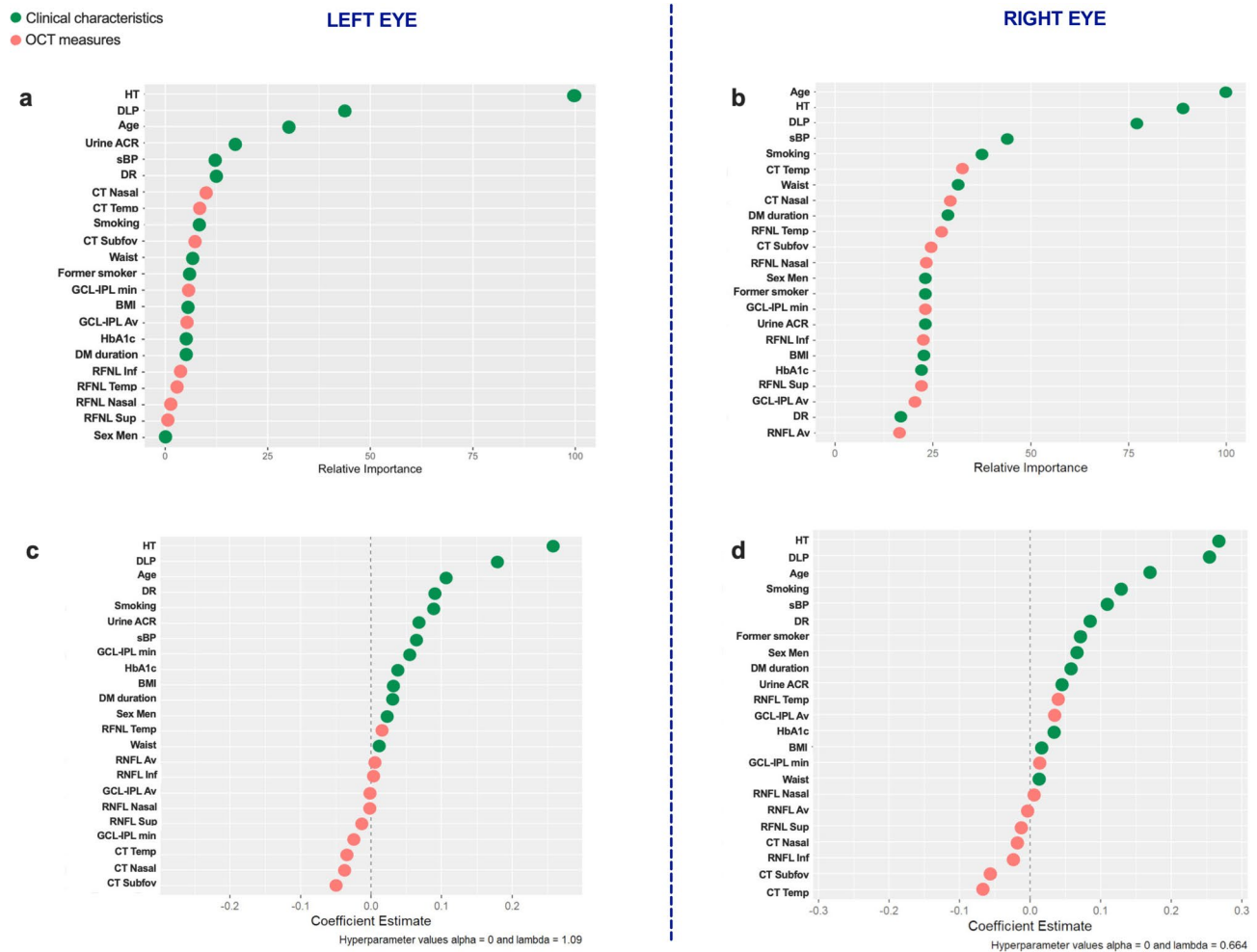


Fig. 3. (a) and (b) Plots ranking the feature's importance in the prediction of carotid plaque by the Random Forest machine learning model, where the x-axis represents the relative importance value and the y-axis the features ranked in descending order of importance. c and d) Plots displaying the standardized coefficient estimates. Positive values indicate a positive association with the presence of carotid plaque. Pink dots represent clinical features, and green dots ophthalmological measures.

with caution and confirmed in larger, prospective studies to ensure their validity and generalizability. Thirdly, despite excluding patients with refractive errors ≥ 5.0 diopters, the omission of recording axial length, a known influencer of chorioretinal thickness, represents a limitation. Additionally, while we excluded patients with significant diabetic nephropathy, we did not exclude those with DR, which may have introduced microvascular influences on choroidal thickness, potentially confounding the relationship between choroidal thickness and carotid plaques. Fourthly, one significant limitation of our study is that we used average retinal and choroidal thickness as surrogate markers for subclinical atherosclerosis without directly assessing plaque size or degree of stenosis in the carotid arteries. This should be considered when interpreting our findings, as smaller plaques may have a limited impact on post-stenotic circulation. Another limitation is the potential confounding effect of hypertension on choroidal thickness, given its higher prevalence in the carotid plaque group compared to the no plaque group (55% vs. 12%). A reduction in choroidal thickness has been consistently observed in hypertensive adults compared to normotensive controls⁷². While including hypertension as a feature in our model helps control for its effect and ensures that it distinguishes between its impact on choroidal thickness and the presence of carotid plaques, our feature importance analysis indicated that hypertension and age were the most significant variables for making accurate predictions. The regularized regression models showed that hypertension had the highest coefficient estimate, suggesting it heavily influences the model's predictions. Consequently, the significant influence of hypertension indicates that the model might partially be predicting hypertension rather than solely subclinical carotid plaques. To address this concern, additional analyses should be conducted where the models are trained and tested separately on hypertensive and non-hypertensive cohorts to observe any differences in the predictive value of choroidal thickness. Without this approach, we cannot completely rule out the possibility that the model's predictions are influenced by hypertension. Fifthly, the sensitivity of the model was not exceptionally high, potentially leading to some omissions when employed as a screening tool. We anticipate that enhancing the overall performance of predictive models could be achieved through the incorporation of more extensive

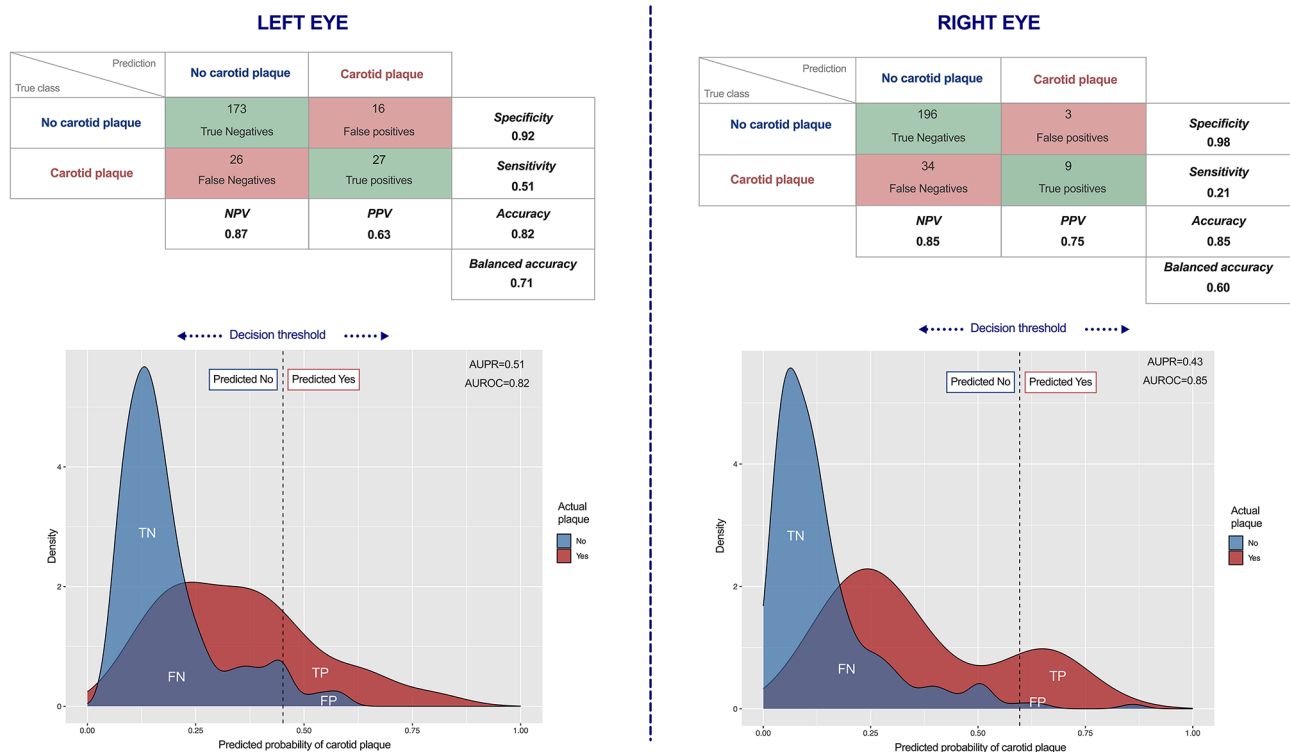


Fig. 4. Confusion matrices and performance plots illustrating the predictive performance of the models in determining the presence of carotid plaque. AUPR, area under the precision-recall curve; AUROC, area under the receiver-operating characteristic curve; NPV, negative predictive value; PPV, positive predictive value.

training data from multicenter studies involving different hospitals (and different countries) to ensure that the performance assessment results are as broadly applicable as possible. Furthermore, the relatively limited set of features employed in the prediction models might impact their universality, given that a more extensive array of features generally contributes to a more accurate model.

Conclusion

Patients with T1DM are typically monitored by an ophthalmologist to identify any signs of diabetes-associated eye complications, such as DR. Our study shows that those with subclinical plaques also experience a significant reduction in choroidal thickness, suggesting that it could serve as an additional early marker of CV risk. While traditional risk factors such as age, hypertension, dyslipidemia, smoking, and DR remain more strongly associated with subclinical carotid plaques, integrating choroidal thickness measurement via OCT can provide incremental value in specific clinical contexts. This measure could complement standard risk assessments and help identify individuals needing additional cardiovascular evaluations, particularly in endocrinology and ophthalmology settings where patients are already undergoing regular eye exams. However, the cost and practicality of OCT imaging should be considered, and further investigations are necessary to confirm its reliability and consistency. Rigorous validation studies involving larger and more diverse patient cohorts are required to establish generalizability and ensure the robustness and applicability of this measure in clinical settings. Future studies should include detailed imaging of the carotid artery and measurement of atherosclerotic plaque characteristics (e.g., plaque composition, volume, and stability) to better understand the relationship between the choroid and carotid artery atherosclerosis. Moreover, conducting longitudinal studies to track changes over time would help establish causal relationships and the predictive value of choroid changes for cardiovascular events. Despite needing external validation, our study comprehensively explored OCT measures in predicting carotid plaques in T1DM, with machine-learning insights offering potential biomarkers for subclinical atherosclerosis.

Data availability

Some or all datasets generated during and/or analyzed during the current study are not publicly available but are available from the corresponding author upon reasonable request.

Received: 5 September 2024; Accepted: 7 March 2025

Published online: 11 March 2025

References

1. Wagenknecht, L. E. et al. Diabetes and progression of carotid atherosclerosis. *Arterioscler. Thromb. Vasc. Biol.* **23**, 1035–1041 (2003).

2. Morrish, N. J., Wang, S. L., Stevens, L. K., Fuller, J. H. & Keen, H. Mortality and causes of death in the WHO multinational study of vascular disease in diabetes. *Diabetologia* **44** (Suppl 2), S14–21 (2001).
3. Jenkins, A., Januszewski, A. & O'Neal, D. The early detection of atherosclerosis in type 1 diabetes: Why, how and what to do about it. *Cardiovasc. Endocrinol. Metab.* **8**, 14–27 (2019).
4. Herrington, W., Lacey, B., Sherliker, P., Armitage, J. & Lewington, S. Epidemiology of atherosclerosis and the potential to reduce the global burden of atherothrombotic disease. *Circ. Res.* **118**, 535–546 (2016).
5. Wong, N. D. et al. Atherosclerotic cardiovascular disease risk assessment: An American Society for Preventive Cardiology clinical practice statement. *Am. J. Prev. Cardiol.* **10**, 100335 (2022).
6. Williams, K. J. Eradicating atherosclerotic events by targeting early subclinical disease: It is time to retire the therapeutic paradigm of too much, too late. *Arterioscler. Thromb. Vasc. Biol.* **44**, 48–64 (2024).
7. Sillesen, H. et al. Carotid plaque burden as a measure of subclinical atherosclerosis: Comparison with other tests for subclinical arterial disease in the high risk plaque bioimage study. *JACC Cardiovasc. Imaging* **5**, 681–689 (2012).
8. Baber, U. et al. Prevalence, impact, and predictive value of detecting subclinical coronary and carotid atherosclerosis in asymptomatic adults: The bioimage study. *J. Am. Coll. Cardiol.* **65**, 1065–1074 (2015).
9. Katakami, N., Matsuoka, T. A. & Shimomura, I. Clinical utility of carotid ultrasonography: Application for the management of patients with diabetes. *J. Diabetes Investig.* **10**, 883–898 (2019).
10. Viswanathan, V. et al. Low-cost preventive screening using carotid ultrasound in patients with diabetes. *Front. Biosci.* **25**, 1132–1171 (2020).
11. Giannopoulou, E. Z. et al. Subclinical arterial damage in children and adolescents with type 1 diabetes: A systematic review and meta-analysis. *Pediatr. Diabetes* **20**, 668–677 (2019).
12. Arthur, A., Alexander, A., Bal, S., Sivadasan, A. & Aaron, S. Ophthalmic masquerades of the atherosclerotic carotids. *Indian J. Ophthalmol.* **62**, 472–476 (2014).
13. Kur, J., Newman, E. A. & Chan-Ling, T. Cellular and physiological mechanisms underlying blood flow regulation in the retina and choroid in health and disease. *Prog Retin Eye Res.* **31**, 377–406 (2012).
14. Kiel, J. W. *In the Ocular Circulation Ch. Chapter 2* (Morgan & Claypool Life Sciences, 2010).
15. Thomas, D. & Duguid, G. Optical coherence tomography—a review of the principles and contemporary uses in retinal investigation. *Eye* **18**, 561–570 (2004).
16. Yeung, S. C., You, Y., Howe, K. L. & Yan, P. Choroidal thickness in patients with cardiovascular disease: A review. *Surv. Ophthalmol.* **65**, 473–486 (2020).
17. El-Fayoumi, D., Badr Eldine, N. M., Esmail, A. F., Ghalwash, D. & Soliman, H. M. Retinal nerve fiber layer and ganglion cell complex thicknesses are reduced in children with type 1 diabetes with no evidence of vascular retinopathy. *Invest. Ophthalmol. Vis. Sci.* **57**, 5355–5360 (2016).
18. Gundogan, F. C. et al. Early neurodegeneration of the inner retinal layers in type 1 diabetes mellitus. *Ophthalmologica* **235**, 125–132 (2016).
19. Bialosterski, C. et al. Decreased optical coherence tomography-measured pericentral retinal thickness in patients with diabetes mellitus type 1 with minimal diabetic retinopathy. *Br. J. Ophthalmol.* **91**, 1135–1138 (2007).
20. Pinilla, I. et al. Changes in total and inner retinal thicknesses in type 1 diabetes with no retinopathy after 8 years of follow-up. *Retina* **40**, 1379–1386 (2020).
21. Yu, Q. et al. Two-year longitudinal study on changes in thickness of the retinal nerve fiber layer and ganglion cell layer in children with type 1 diabetes mellitus without visual impairment or diabetic retinopathy. *Curr. Eye Res.* **47**, 1218–1225 (2022).
22. van Dijk, H. W. et al. Selective loss of inner retinal layer thickness in type 1 diabetic patients with minimal diabetic retinopathy. *Invest. Ophthalmol. Vis. Sci.* **50**, 3404–3409 (2009).
23. van Dijk, H. W. et al. Decreased retinal ganglion cell layer thickness in patients with type 1 diabetes. *Invest. Ophthalmol. Vis. Sci.* **51**, 3660–3665 (2010).
24. Karti, O. et al. Retinal ganglion cell loss in children with type 1 diabetes mellitus without diabetic retinopathy. *Ophthalmic Surg. Lasers Imaging Retina* **48**, 473–477 (2017).
25. Carbonell, M. et al. Assessment of inner retinal layers and choroidal thickness in type 1 diabetes mellitus: A cross-sectional study. *J. Clin. Med.* **8** (2019).
26. Gołębiewska, J. et al. Choroidal thickness and ganglion cell complex in pubescent children with type 1 diabetes without diabetic retinopathy analyzed by spectral domain optical coherence tomography. *J. Diabetes Res.* **2018**, 5458015 (2018).
27. Bayat, A. H., Cakir, A., Bezen, D. & Elcioglu, M. N. Subfoveal choroidal thickness and ganglion cell complex in children with type 1 diabetes mellitus without diabetic retinopathy. *Beyoglu Eye J.* **5**, 174–177 (2020).
28. Sayin, N. et al. Evaluation of subfoveal choroidal thickness in children with type 1 diabetes mellitus: An EDI-OCT study. *Semin Ophthalmol.* **29**, 27–31 (2014).
29. Ermerak, B. C. et al. Evaluation of choroidal thickness in children with type 1 diabetes: The role of optical coherence tomography in diabetic retinopathy screening. *Clin. Pediatr. Endocrinol.* **30**, 41–47 (2021).
30. Kinoshita, T. et al. Systemic and ocular determinants of choroidal structures on optical coherence tomography of eyes with diabetes and diabetic retinopathy. *Sci. Rep.* **9**, 16228 (2019).
31. Yolcu, U. et al. Choroidal and macular thickness changes in type 1 diabetes mellitus patients without diabetic retinopathy. *Postgrad. Med.* **128**, 755–760 (2016).
32. Esmaeelpour, M. et al. Choroidal thinning in diabetes type 1 detected by 3-dimensional 1060 Nm optical coherence tomography. *Invest. Ophthalmol. Vis. Sci.* **53**, 6803–6809 (2012).
33. Peña, A. S. et al. Early atherosclerosis is associated with retinal microvascular changes in adolescents with type 1 diabetes. *Pediatr. Diabetes* **19**, 1467–1470 (2018).
34. Carbonell, M. et al. Diabetic retinopathy is associated with the presence and burden of subclinical carotid atherosclerosis in type 1 diabetes. *Cardiovasc. Diabetol.* **17**, 66 (2018).
35. Levey, A. S. et al. A new equation to estimate glomerular filtration rate. *Ann. Intern. Med.* **150**, 604–612 (2009).
36. Wilkinson, C. P. et al. Proposed international clinical diabetic retinopathy and diabetic macular edema disease severity scales. *Ophthalmology* **110**, 1677–1682 (2003).
37. Boonarpa, N. et al. Standardization of choroidal thickness measurements using enhanced depth imaging optical coherence tomography. *Int. J. Ophthalmol.* **8**, 484–491 (2015).
38. Alonso, N., Moliner, P. & Mauricio, D. Pathogenesis, clinical features and treatment of diabetic cardiomyopathy. *Adv. Exp. Med. Biol.* **1067**, 197–217 (2018).
39. Touboul, P. J. et al. Mannheim carotid intima-media thickness and plaque consensus (2004–2006–2011). An update on behalf of the advisory board of the 3rd, 4th and 5th watching the risk symposia, at the 13th, 15th and 20th European stroke conferences, Mannheim, Germany, 2004, Brussels, Belgium, 2006, and Hamburg, Germany, 2011. *Cerebrovasc. Dis.* **34**, 290–296 (2012).
40. van Buuren, S. & Groothuis-Oudshoorn, K. Mice: Multivariate imputation by chained equations in R. *J. Stat. Softw.* **45**, 1–67 (2011).
41. Couronne, R., Probst, P. & Boulesteix, A. L. Random forest versus logistic regression: A large-scale benchmark experiment. *BMC Bioinform.* **19**, 270 (2018).
42. Tohka, J. & van Gils, M. Evaluation of machine learning algorithms for health and wellness applications: A tutorial. *Comput. Biol. Med.* **132**, 104324 (2021).

43. Varoquaux, G. & Colliot, O. in *Machine Learning for Brain Disorders* (ed Olivier Colliot) 601–630 (Springer, 2023).
44. Aguilera, E. et al. Low prevalence of subclinical atherosclerosis in asymptomatic patients with type 1 diabetes in a European mediterranean population. *Diabetes Care*. **37**, 814–820 (2014).
45. Distiller, L. A., Joffe, B. I., Melville, V., Welman, T. & Distiller, G. B. Carotid artery intima-media complex thickening in patients with relatively long-surviving type 1 diabetes mellitus. *J. Diabetes Complicat.* **20**, 280–284 (2006).
46. Ogawa, Y., Uchigata, Y. & Iwamoto, Y. Progression factors of carotid intima-media thickness and plaque in patients with long-term, early-onset type 1 diabetes mellitus in Japan: Simultaneous comparison with diabetic retinopathy. *J. Atheroscler Thromb.* **16**, 821–828 (2009).
47. Song, P. et al. Global and regional prevalence, burden, and risk factors for carotid atherosclerosis: A systematic review, meta-analysis, and modelling study. *Lancet Glob Health*. **8**, e721–e729 (2020).
48. Larsen, J. et al. Silent coronary atheromatosis in type 1 diabetic patients and its relation to long-term glycemic control. *Diabetes* **51**, 2637–2641 (2002).
49. Pezeshki Rad, M., Farrokhi, D., Vakili, R., Omidbakhsh, M. & Mohammadi, M. The association between carotid Intima-Media thickness and the duration of type 1 diabetes in children. *Iran. J. Pediatr.* **24**, 249–254 (2014).
50. Abdelghaffar, S., Amir, E., Hadidi, M. E., El Mougi, F. & A. Carotid intima-media thickness: An index for subclinical atherosclerosis in type 1 diabetes. *J. Trop. Pediatr.* **52**, 39–45 (2006).
51. Kupfer, R. et al. Predictors of subclinical atherosclerosis evaluated by carotid intima-media thickness in asymptomatic young women with type 1 diabetes mellitus. *Arch. Endocrinol. Metab.* **61**, 115–121 (2017).
52. Orchard, T. J. et al. Insulin resistance-related factors, but not glycemia, predict coronary artery disease in type 1 diabetes: 10-year follow-up data from the Pittsburgh epidemiology of diabetes complications study. *Diabetes Care*. **26**, 1374–1379 (2003).
53. Araszkiewicz, A. et al. Neurodegeneration of the retina in type 1 diabetic patients. *Pol. Arch. Med. Wewn.* **122**, 464–470 (2012).
54. Elhabashy, S. A., Elbarbary, N. S., Nageb, K. M. & Mohammed, M. M. Can optical coherence tomography predict early retinal microvascular pathology in type 1 diabetic adolescents without minimal diabetic retinopathy? A single-centre study. *J. Pediatr. Endocrinol. Metab.* **28**, 139–146 (2015).
55. Ciresi, A. et al. OCT is not useful for detection of minimal diabetic retinopathy in type 1 diabetes. *Acta Diabetol.* **47**, 259–263 (2010).
56. van de Kreeke, J. A. et al. The Spatial relation of diabetic retinal neurodegeneration with diabetic retinopathy. *PLoS ONE*. **15**, e0231552 (2020).
57. Delaey, C. & van de Voorde, J. Regulatory mechanisms in the retinal and choroidal circulation. *Ophthalmic Res.* **32**, 249–256 (2000).
58. Akca Bayar, S. et al. Structural analysis of the retina and choroid before and after carotid artery surgery. *Curr. Eye Res.* **45**, 496–503 (2020).
59. Zhou, S. W. et al. The impact of carotid endarterectomy on choriocapillaris perfusion. *Invest. Ophthalmol. Vis. Sci.* **64**, 42 (2023).
60. Chahine, Y. et al. Machine learning and the conundrum of stroke risk prediction. *Arrhythm. Electrophysiol. Rev.* **12**, e07 (2023).
61. Bin, C. et al. Machine learning models for predicting the risk factor of carotid plaque in cardiovascular disease. *Front. Cardiovasc. Med.* **10**, 1178782 (2023).
62. Fan, J. et al. The prediction of asymptomatic carotid atherosclerosis with electronic health records: A comparative study of six machine learning models. *BMC Med. Inf. Decis. Mak.* **21**, 115 (2021).
63. Yu, J. et al. Machine learning models for screening carotid atherosclerosis in asymptomatic adults. *Sci. Rep.* **11**, 22236 (2021).
64. Kim, J. H. et al. Relationship between coronary artery calcification and central chorioretinal thickness in patients with subclinical atherosclerosis. *Ophthalmologica* **244**, 18–26 (2021).
65. Turan-Vural, E. & Vural, U. Evaluation of peripapillary and subfoveal choroid thickness in asymptomatic carotid artery stenosis. *Clin. Ophthalmol.* **14**, 1641–1650 (2020).
66. Ahmad, M., Kaszubski, P. A., Cobbs, L., Reynolds, H. & Smith, R. T. Choroidal thickness in patients with coronary artery disease. *PLoS ONE*. **12**, e0175691 (2017).
67. Jiang, C. Q. et al. An overview of the Guangzhou biobank cohort study-cardiovascular disease subcohort (GBCS-CVD): A platform for multidisciplinary collaboration. *J. Hum. Hypertens.* **24**, 139–150 (2010).
68. Drinkwater, J. J., Davis, T. M. E. & Davis, W. A. The relationship between carotid disease and retinopathy in diabetes: A systematic review. *Cardiovasc. Diabetol.* **19**, 54 (2020).
69. István, L. et al. Imaging retinal microvascular manifestations of carotid artery disease in older adults: From diagnosis of ocular complications to Understanding microvascular contributions to cognitive impairment. *Geroscience* **43**, 1703–1723 (2021).
70. Bradley, S. M. et al. Patient selection for diagnostic coronary angiography and Hospital-Level percutaneous coronary intervention appropriateness: Insights from the National cardiovascular data registry. *JAMA Intern. Med.* **174**, 1630–1639 (2014).
71. Johri, A. M. et al. Recommendations for the assessment of carotid arterial plaque by ultrasound for the characterization of atherosclerosis and evaluation of cardiovascular risk: From the American society of echocardiography. *J. Am. Soc. Echocardiogr.* **33**, 917–933 (2020).
72. Papathanasiou, K. A. et al. Choroidal thickness in patients with systemic arterial hypertension: A systematic review and meta-analysis. *Ther. Adv. Ophthalmol.* **14**, 25158414221132825 (2022).

Acknowledgements

We want to acknowledge particularly the participants and the IGTP-HUGTP (B.0000643) and IRBLleida (B.0000682) Biobanks integrated into the PLATAFORMA BIOBANCOS (PT20/00050 and PT20/00021, respectively).

Author contributions

Conceptualization: D.M. and J.F.-N.; Methodology: E.C., M.C., D.M. and J.F.-N.; Investigation: I.S.-M., M.C., A.T., M.H., and N.A.; Formal analysis: E.C. and E.C.; Writing—original draft: E.C., M.G., M.C. and E.C.; Supervision: D.M. and J. F.-N. All authors reviewed the manuscript.

Declarations

Competing interests

The authors declare no competing interests.

Additional information

Supplementary Information The online version contains supplementary material available at <https://doi.org/10.1038/s41598-025-93534-z>.

Correspondence and requests for materials should be addressed to D.M.

Reprints and permissions information is available at www.nature.com/reprints.

Publisher's note Springer Nature remains neutral with regard to jurisdictional claims in published maps and institutional affiliations.

Open Access This article is licensed under a Creative Commons Attribution-NonCommercial-NoDerivatives 4.0 International License, which permits any non-commercial use, sharing, distribution and reproduction in any medium or format, as long as you give appropriate credit to the original author(s) and the source, provide a link to the Creative Commons licence, and indicate if you modified the licensed material. You do not have permission under this licence to share adapted material derived from this article or parts of it. The images or other third party material in this article are included in the article's Creative Commons licence, unless indicated otherwise in a credit line to the material. If material is not included in the article's Creative Commons licence and your intended use is not permitted by statutory regulation or exceeds the permitted use, you will need to obtain permission directly from the copyright holder. To view a copy of this licence, visit <http://creativecommons.org/licenses/by-nc-nd/4.0/>.

© The Author(s) 2025